Regulation of β-Sheet Structures within Amyloid-Like β-Sheet Assemblage from Tripeptide Derivatives

Norihiro Yamada,*,† Katsuhiko Ariga,‡ Masanobu Naito,† Kazuhiro Matsubara,† and Emiko Koyama†,§

Contribution from the Faculty of Education, Chiba University, 1-33 Yayoi-cho, Inage-ku, Chiba 263-8522, Japan, and Graduate School of Materials Science, Nara Institute of Science and Technology (NAIST), 8916-5 Takayama, Ikoma, Nara 630-0101, Japan

Received April 20, 1998

Abstract: *N*-(11-Trimethylammonioundecanoyl)-*O*,*O*′-didodecyl tripeptide bromides and *N*-(11-trimethylammonioundecanyl)-*O*-dodecyl tripeptide bromides formed a parallel β-sheet structure when they aggregated in water and in CCl_4. The parallel β-sheet was distinguished from the antiparallel counterpart by Fourier transform infrared spectroscopy because the former lacks a weak band at about 1690 cm^{-1} that is characteristic for the latter. The FT-IR spectra of the aggregate in CCl_4 remained unchanged if the solution was diluted to 0.01 mM, condensed to dryness, or heated to 60 °C, and hence, the β-sheet was easily formed and thermodynamically stable. The parallel β-sheet was also possible to transform into an antiparallel β-sheet, for example, by mixing with another tripeptide-containing amphiphile whose tripeptide part had an opposite direction. Transmission electron microscope (TEM) and atomic force microscope (AFM) pictures revealed that the aggregate in CCl_4 is a bundle of small filaments whose diameters are 70−80 Å. Developed interpeptide hydrogen bonding should be formed along the long axis of the filament. The morphological structures and stable peptide arrangements of the present assemblages are similar to those of the amyloid fiber whose accumulation causes fatal diseases.

Inappropriate mutation of normal cellular proteins generates fragmentary peptides or abnormal disease-causing isoforms (prion peptides).[1] The small peptides sometimes self-assemble into an amyloid fibril, which accumulates in various internal organs and causes functional diseases called amyloidosis. Because the prion and the amyloid contain a rich amount of β-sheet structure, it is important to constitute a β-sheet assemblage to understand the pathogenesis and the therapeutics of these diseases. In this regard, we can find several model studies on oligopeptides, for example, leucine-rich repeat oligopeptides[2] and ionic self-complementary oligopeptides.[3] Aggeli suspects that all of the gel-forming oligopeptides could also be applied to the amyloid model.[4] However, it is not easy to prepare the oligopeptide forming a desired secondary structure, because all of the oligopeptides adopt an inherent secondary structure depending on the kinds of component amino acids and their number.

In this paper, we report a new class of an amyloid model using tripeptide derivatives shown in Chart 1. Because all of the derivatives except for **8** formed an aggregate not only in water but also in some nonpolar organic solvents,[5−7] they should pack according to a bilayer structure (Figure 1a and b) or an interdigitated monolayer structure (Figure 1c) when they aggregate.[8] The former should produce a parallel β-sheet structure, whereas the latter should form either a parallel or an antiparallel β-sheet structure. On the other hand, an antiparallel β-sheet would be predominantly formed if the two kinds of molecules whose tripeptides had opposite directions were mixed with each other. Thus, a highly ordered β-sheet structure which is the characteristic property of the amyloid should be available from the simple tripeptides.

Using Fourier transform infrared (FT-IR) spectroscopy, we examined the detailed structure of the hydrogen bonding in the assemblage of amphiphilic and hydrophobic tripeptide derivatives. Morphological similarity between the assemblage and the amyloid was also studied using a transmission electron microscope (TEM) and an atomic force microscope (AFM).

Experimental Section

Synthesis of Tripeptide Derivatives. *N-tert*-Butyloxycarbonyl-L-amino acids (Boc-L-amino acids) were purchased from Calbiochem-Novabiochem International, Inc., and 11-bromoundecanoic acid and diethyl phosphorocyanidate (DEPC) from Wako Pure Chemical Ind., Ltd. All of the melting points were recorded on Yanaco micromelting apparatus (MP-S3) and are uncorrected. The IR spectra were obtained on a JASCO IRA-1 infrared spectrophotometer for the intermediates and on a Nicolet 740 Fourier transform infrared (FT-IR) spectrophometer for the final compounds according to the method described later. Chemical shifts of the ^1H NMR spectra were recorded on a Hitachi R600 (60 MHz) or a JEOL GSX500 (500 MHz) spectrometer and are given relative to tetramethylsilane (δ 0.00). All reactions were

† Chiba University.

‡ Nara Institute of Science and Technology.

§ Present Address: Department of Chemistry, University of Tsukuba, Tsukuba, Ibaraki 305-8751, Japan.

(1) Prusiner, S. B. *Science* **1997**, *278*, 245−251.

(2) Symmons, M. F.; Buchanan, S. G. St. C.; Clarke, D. T.; Jones, G.; Gay, N. J. *FEBS Lett.* **1997**, *412*, 397−403,.

(3) Zhang, S.; Rich, A. *Proc. Natl. Acad. Sci. U.S.A.* **1997**, *94*, 23−28.

(4) Aggeli, A.; Bell, M.; Boden, N.; Keen, J. N.; Knowles, P. F.; McLeish, T. C. B.; Pitkeathly, M.; Radford, S. E. *Nature* **1997**, *386*, 259−262.

(5) Yamada, N.; Koyama, E.; Kaneko, M.; Seki, H.; Ohtsu, H.; Furuse, T. *Chem. Lett.* **1995**, 387−388.

(6) Yamada, N.; Koyama, E.; Imai, T.; Matsubara, K.; Ishida, S. *J. Chem. Soc., Chem. Commun.* **1996**, 2297−2298.

(7) Yamada, N.; Koyama, E.; Maruyama, K. *Kobunshi Ronbunshu* **1995**, *52*, 629−638.

(8) Kunitake, T. *Angew Chem., Int. Ed. Engl.* **1992**, *31*, 709−726.

10.1021/ja981363q CCC: $15.00
Published on Web 11/11/1998

Chart 1

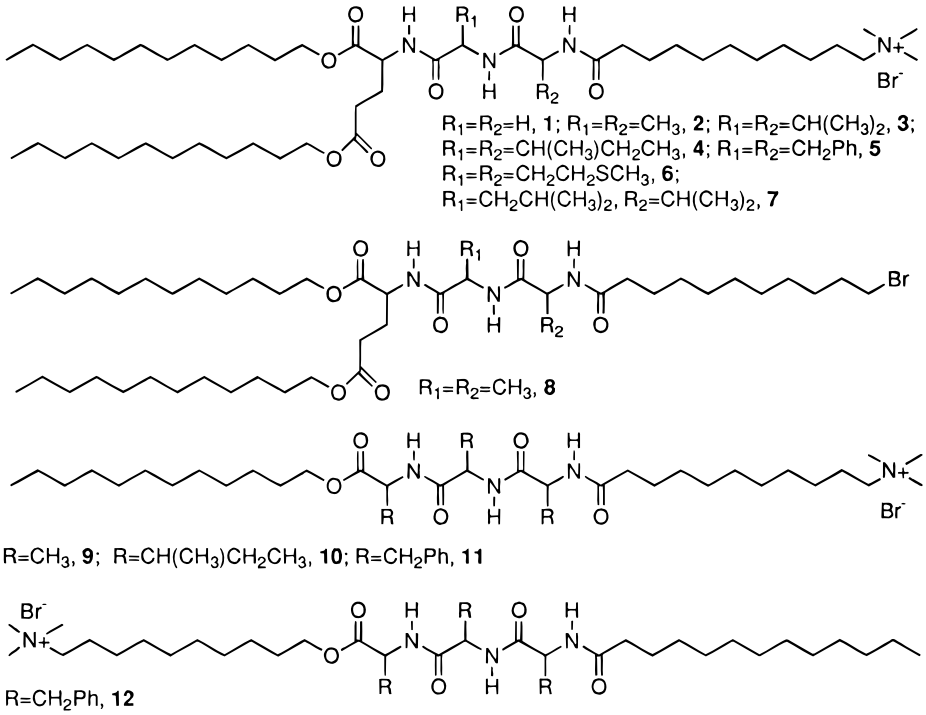

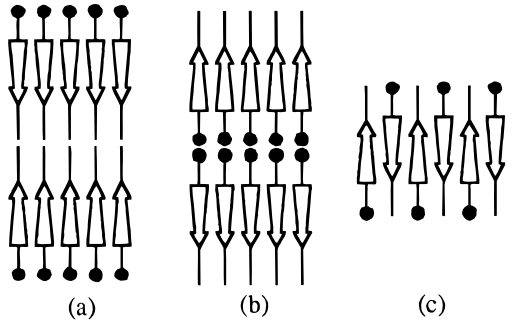

Figure 1. Different possibilities of arranging tripeptide-containing molecules. (a) Aqueous bilayer structure with a single component. (b) Reversed bilayer structure with a single component in organic media. (c) Interdigitated monolayer structure with a single component either in water or in organic media.

monitored by thin-layer chromatography (Merck TLC aluminum sheet silica gel 60 GF_{254}; developer, 10:1 chloroform−methanol). Elemental analyses (C, H, and N) were performed at the Analysis Center, Chiba University.

The double-chain, tripeptide-containing amphiphiles **1**−**7** were prepared by a stepwise condensation of Boc-L-amino acid to didodecyl-L-glutamate. The following method was used for the synthesis of **2** and **8** (an intermediate of **2**) which is the general synthetic procedure.

***N*-[*N*-[*N*-(11-Bromoundecanoyl)-L-alanyl]-L-alanyl]-*O*,*O*′-didodecyl-L-glutamate (8).** Into a mixture of didodecyl-L-glutamate hydrochloride[9] (3.00 g, 5.77 mmol) and Boc-L-Ala-OH (1.14 g, 6.00 mmol) in 50 mL of dry THF was added Et_3N (0.61 g, 6.03 mmol) at once. Et_3N·HCl immediately precipitated. To the mixture was added a solution of diethyl phosphorocyanidate (0.98 g, 6.01 mmol) in 30 mL of dry THF within 15 min with stirring at a temperature below 5 °C. The mixture was allowed to stand overnight at room temperature and was filtered and evaporated to dryness in vacuo. The residual oil was dissolved in chloroform, washed three times with saturated sodium hydrogen carbonate and with saltwater, evaporated, and recrytallized from a methanol−water mixture to give a colorless powder (Boc-Ala-Glu($OC_{12}H_{25}$)$_2$, 3.57 g, 95%): mp 42.0−45.0 °C; TLC R_f 0.40 (one spot); IR (CCl_4 past) ν(N−H) 3380, 3280 cm^{-1}, $\nu_{as}(CH_2)$ 2920 cm^{-1}, $\nu_s(CH_2)$ 2840 cm^{-1}, ν(C═O, ester) 1740 cm^{-1}, ν(C═O, urethane) 1710 cm^{-1}, ν(C═O, amide I) 1680 cm^{-1}, δ(N−H, amide II) 1530 cm^{-1}, ν(C−C−O, ester) 1180 cm^{-1}.

To the solution of Boc-Ala-Glu($OC_{12}H_{25}$)$_2$ (2.90 g, 4.43 mmol) in 10 mL of dichloromethane was added 28.7 g of 25% HBr−acetic acid at once under stirring with ice cooling. After gas evolution ended (4 hs), the mixture was neutralized with saturated sodium hydrogen carbonate with ice cooling. The mixture was poured into chloroform, washed three times with saturated sodium hydrogen carbonate and with saltwater, dried over dry magnesium sulfate, and evaporated to dryness in vacuo. The residual oil was solidified in a freezer and was recrystallized from petroleum ether to give a colorless powder (H-Ala-Glu($OC_{12}H_{25}$)$_2$, 1.90 g, 77%): mp 41.0−45.0 °C; TLC R_f 0.30 (one spot); IR (CCl_4 past) ν(N−H) 3600−3200 cm^{-1} (broad), $\nu_{as}(CH_2)$ 2940 cm^{-1}, $\nu_s(CH_2)$ 2840 cm^{-1}, ν(C═O, ester) 1750 cm^{-1}, ν(C═O, amide I) 1680 cm^{-1}, δ(N−H, amide II) 1540 cm^{-1}. The bands attributed to the urethane linkage completely disappeared.

Into a mixture of H-Ala-Glu($OC_{12}H_{25}$)$_2$ (1.80 g, 3.24 mmol) and Boc-L-Ala-OH (0.66 g, 3.49 mmol) in 50 mL of dry THF was added Et_3N (0.35 g, 3.50 mmol) at once. Et_3N·HCl immediately precipitated. To the mixture was added a solution of diethyl phosphorocyanidate (0.57 g, 3.50 mmol) in 30 mL of dry THF within 15 min with stirring at a temperature below 5 °C. The mixture was allowed to stand overnight at room temperature and was filtered and evaporated to dryness in vacuo. The residual oil was dissolved in chloroform, washed three times with saturated sodium hydrogen carbonate, washed with saltwater, and evaporated. The residue (Boc-Ala-Ala-Glu($OC_{12}H_{25}$)$_2$) was not solidified and was used without further purification, because the TLC result (R_f 0.41, one spot) indicated the presence of no other components: IR (neat) ν(N−H) 3440, 3340 cm^{-1}, $\nu_{as}(CH_2)$ 2940 cm^{-1}, $\nu_s(CH_2)$ 2860 cm^{-1}, ν(C═O, ester) 1740 cm^{-1}, ν(C═O, urethane) 1720 cm^{-1}, ν(C═O, amide I) 1680 cm^{-1}, δ(N−H, amide II) 1530 cm^{-1}, ν(C−C−O, ester) 1180 cm^{-1}.

Into a mixture of the Boc-Ala-Ala-Glu($OC_{12}H_{25}$)$_2$ (2.35 g, 3.23 mmol) in 10 mL of dichloromethane was added 15.3 g of 25% HBr−acetic acid was added at once under stirring with ice cooling. After gas evolution ended (3 hs), the mixture was neutralized with saturated sodium hydrogen carbonate with ice cooling. The mixture was poured into chloroform, washed three times with saturated sodium hydrogen carbonate and with saltwater, dried over dry magnesium sulfate, and evaporated to dryness in vacuo. A colorless oil was obtained (H-Ala-

(9) Kunitake, T.; Nakashima, N.; Hayashida, S.; Yonemori. K. *Chem. Lett.* **1979**, 1413−1416.

Ala-Glu($OC_{12}H_{25}$)$_2$, 1.87 g, 93%): TLC R_f 0.43; IR (neat) ν(N−H) 3260 cm^{-1}, ν_{as}(CH_2) 2920 cm^{-1}, ν_s(CH_2) 2840 cm^{-1}, ν(C═O, ester) 1740 cm^{-1}, ν(C═O, amide I) 1640 cm^{-1}, δ(N−H, amide II) 1540 cm^{-1}. The IR spectra contained no Boc-Ala-Ala-Glu($OC_{12}H_{25}$)$_2$, and TLC indicated that no other impurity was included; hence, the material was used in the next synthesis without further purification.

Into a mixture of H-Ala-Ala-Glu($OC_{12}H_{25}$)$_2$ (1.87 g, 2.99 mmol) and 11-bromoundecanoic acid (0.95 g, 3.95 mmol) in 30 mL of dry THF was added Et_3N (0.36 g, 3.59 mmol) at once. To the mixture was added a solution of diethyl phosphorocyanidate (0.58 g, 3.59 mmol) in 30 mL of dry THF within 15 min with stirring at a temperature below 5 °C. The mixture was allowed to stand overnight at room temperature, filtered, dried over dry magnesium sulfate, and evaporated to dryness in vacuo. The residual solids were dissolved in chloroform, washed with saltwater, evaporated, and recrytallized twice from methanol to give a colorless powder **8** (1.66 g, 64%): mp 85.5−87.5 °C; TLC R_f 0.66; IR (10 mM of CCl_4 solution) ν(N−H) 3281 cm^{-1}, ν_{as}(CH_2) 2928 cm^{-1}, ν_s(CH_2) 2853 cm^{-1}, ν(C═O, ester, see Figure 2) 1738 cm^{-1}, ν(C═O, amide I, see Figure 2) 1630 and 1688 cm^{-1}, δ(N−H, amide II, see Figure 2) 1527 cm^{-1}; ^{1}H NMR (60 MHz, $CDCl_3$) δ 0.90 (brt, 6H, 2CH_3 in long chain) 1.05−1.80 (brm, 60H, 27CH_2 in long chain and 2CH_3 in Ala), 1.87 (brs, *C*H_2CH$_2$Br), 2.00−2.60 (brm, 6H, NCOCH_2 and OCO*C*H_2*C*H_2 in Glu), 3.41 (t, J = 7 Hz, 2H, CH_2Br), 3.90−4.30 (m, 4H, COOCH_2), 4.30−4.90 (brm, 3H, CH in Ala), 6.43 (d, J = 7 Hz, 1H, NH in Ala), 6.85−7.40 (brm, 2H, NH in Ala and in Glu). Anal. Calcd for $C_{46}H_{86}N_3O_7Br$: C, 63.28; H, 9.93; N, 4.81. Found: C, 63.33; H, 10.31; N, 4.89.

***N*-[*N*-[*N*-(11-Trimethylammonioundecanoyl)-L-alanyl]-L-alanyl]-*O*,*O*′-didodecyl-L-glutamate Bromide (2).** The resultant bromide **8** (1.34 g, 1.87 mmol) was dissolved in 100 mL of dry THF. Dry Me_3N gas was bubbled into the solution under vigorous stirring with ice cooling until the total volume of the solution slightly increased. The flask was stoppered and allowed to stand for 1 week at room temperature in the dark. The solvent and excess Me_3N were removed under reduced pressure. In this procedure, simultaneous use of an amine trap and a hood was required because Me_3N has an extremely bad odor. The residual solid was twice recrystallized from acetone to give a colorless powder (**2**, 1.24 g, 71%): mp 103.5−106.0 °C; TLC R_f 0 (there is no developed component); IR (1 mM of CCl_4 solution) ν(N−H) 3399 cm^{-1}, ν_{as}(CH_2) 2921 cm^{-1}, ν_s(CH_2) 2852 cm^{-1}, ν(C═O, ester, see Figure 2) 1747 and 1728 cm^{-1}, ν(C═O, amide I, see Figure 2) 1647 and 1631 cm^{-1}, δ(N−H, amide II, see Figure 2) 1560 and 1534 cm^{-1}; ^{1}H NMR (500 MHz, $CDCl_3$) δ 0.82 (t, 6H, 2CH_3 in long chain), 1.15−1.40 (brm, 54H, 24CH_2 in long chain and 2CH_3 in Ala), 1.48−1.60 (m, 6H, 2COOCH$_2$*C*H_2 and NCOCH$_2$*C*H_2), 1.77 (brs, 2H, N$^+$-CH$_2$*C*H_2), 1.90−2.10 (m, OCOCH$_2$*C*H_2 in Glu), 2.20 (brs, 2H, NCOCH_2), 2.25−2.40 (m, 2H, OCOCH_2 in Glu), 3.37 (s, 9H, N$^+$(CH_3)$_3$), 3.60 (brs, 2H, N$^+$CH_2), 3.92−4.05 (m, 4H, 2COOCH_2), 4.31−4.37 (m, 1H, CH in Glu), 4.42 (brs, 2H, CH in Ala), 7.44 (brs, 1H, NH in Ala), 7.59 (brs, 1H, NH in Ala), 7.83 (brs, 1H, NH in Glu). Anal. Calcd for $C_{49}H_{95}N_4O_7Br\cdot 1H_2O$: C, 61.94; H, 10.29; N, 5.90. Found: C, 61.92; H, 10.08; N, 5.87.

Other Amphiphiles. Other double-chain, tripeptide-containing amphiphiles **1**, **3**−**7** were prepared in the same manner as that described above. The single-chain, tripeptide-containing amphiphiles **9**−**11** were synthesized using the corresponding dodecyl amino acid instead of didodecyl-L-glutamate, which procedure has been reported elsewhere.[7] The amphiphile **12** whose tripeptide part had an opposite direction was synthesized as follows. 10-Bromodecyloxy-L-phenylalaninate hydrochloride was condensed with Boc-Phe-Phe-OH in the same manner as that described above. After the protection group was removed, the resulting oil was allowed to react with tridecanoic acid, which was followed by quaternization with Me_3N as described above. The analytical data for these final compounds are shown below.

1: recrystallized from acetone; a colorless powder; mp 88.0−91.0 °C; IR (1 mM of CCl_4 solution) ν(N−H) 3366 and 3319 cm^{-1}, ν_{as}(CH_2) 2924 cm^{-1}, ν_s(CH_2) 2852 cm^{-1}, ν(C═O, ester, see Figure 2) 1727 and 1709 cm^{-1}, ν(C═O, amide I, see Figure 2) 1677, 1663 and 1649 cm^{-1}, δ(N−H, amide II, see Figure 2) 1537 and 1513 cm^{-1}; ^{1}H NMR (60 MHz, $CDCl_3$) δ 0.80 (brt, 6H, 2CH_3 in long chain), 1.00−1.65 (brm, 54H, 27CH_2 in long chain), 1.72(brs, 2H, N$^+$CH$_2$*C*H_2), 1.95 (brs, 2H, OCOCH$_2$*C*H_2 in Glu), 2.05−2.50 (brm, 4H, NCOCH_2 and OCOCH_2), 3.20−3.65 (brs, 11H, *C*H_2N$^+$(*C*H_3)$_3$), 3.75−4.20 (brm, 8H, 2COOCH_2 and 2CH_2 in Gly), 4.20−4.75 (brm, 1H, CH in Glu). Anal. Calcd for $C_{47}H_{91}N_4O_7Br\cdot{}^3/_2H_2O$: C, 60.62; H, 10.17; N, 6.02. Found: C, 60.59; H, 10.15; N, 5.77.

3: recrytallized from acetone containing a small amount of ethanol; a colorless powder; mp 191.0−193.5 °C; IR (1 mM of CCl_4 solution) ν(N−H) 3280 cm^{-1}, ν_{as}(CH_2) 2927 cm^{-1}, ν_s(CH_2) 2853 cm^{-1}, ν(C═O, ester, see Figure 4) 1734 cm^{-1}, ν(C═O, amide I, see Figure 4) 1632 cm^{-1}, δ(N−H, amide II, see Figure 4) 1546 cm^{-1}; ^{1}H NMR (60 MHz, $CDCl_3$) δ 0.75−1.05 (br, 18H, 2CH_3 in long chain and 4CH_3 in Val), 1.05−1.85 (brs, 56H, 28CH_2 in long chain), 2.00 (brs, 2H, OCOCH$_2$*C*H_2 in Glu), 1.85−2.45 (brm, 6H, NCOCH_2, OCOCH_2 and 2*C*H(CH_3)$_2$ in Val), 3.30−3.60 (brs, 11H, *C*H_2N$^+$(*C*H_3)$_3$), 3.80−4.20 (brm, 4H, 2COOCH_2), 4.20−4.70 (brm, 3H, 3CH in Glu and Val). Anal. Calcd for $C_{53}H_{103}N_4O_7Br\cdot 2H_2O$: C, 62.64; H, 10.58; N, 5.40. Found: C, 62.40; H, 10.43; N, 5.30.

4: recrytallized from acetone; a colorless powder; mp 180.0−184.0 °C; IR (1 mM of CCl_4 solution) ν(N−H) 3281 cm^{-1}, ν_{as}(CH_2) 2926 cm^{-1}, ν_s(CH_2) 2854 cm^{-1}, ν(C═O, ester, see Figure 4) 1736 cm^{-1}, ν(C═O, amide I, see Figure 4) 1632 cm^{-1}, δ(N−H, amide II, see Figure 4) 1546 cm^{-1}; ^{1}H NMR (60 MHz, $CDCl_3$) δ 0.60−1.05 (br, 18H, 2CH_3 in long chain and 2CH(*C*H_3)CH$_2$*C*H_3 in Ile) 1.10−1.90 (brs, 64H, 29CH_2 in long chain, 2CH(CH$_3$)*C*H_2CH$_3$ in Ile and OCOCH$_2$*C*H_2 in Glu), 2.00−2.60 (br, 6H, OCOCH_2, NCOCH_2 and 2*C*H(CH$_3$)CH$_2$CH$_3$ in Ile), 3.20−3.60 (brs, 11H, *C*H_2N$^+$(*C*H_3)$_3$), 3.80−4.40 (brm, 4H, 2COOCH_2), 4.40−4.70 (brm, 3H, 3CH in Glu and Ile). Anal. Calcd for $C_{55}H_{107}N_4O_7Br\cdot 1H_2O$: C, 63.86; H, 10.62; N, 5.42. Found: C, 63.83; H, 10.56; N, 5.47.

5: recrytallized from acetone; a colorless powder; mp 109.0−111.5 °C; IR (1 mM of CCl_4 solution) ν(N−H) 3282 cm^{-1}, ν_{as}(CH_2) 2925 cm^{-1}, ν_s(CH_2) 2854 cm^{-1}, ν(C═O, ester) 1737 cm^{-1}, ν(C═O, amide I) 1637 cm^{-1}, δ(N−H, amide II) 1542 cm^{-1}; ^{1}H NMR (500 MHz, $CDCl_3$) δ 0.88 (t, J = 7 Hz, 6H, 2CH_3 in long chain), 1.10−1.40 (brm, 48H, 24CH_2 in long chain), 1.51−1.53 (m, 6H, 2COOCH$_2$*C*H_2 and NCOCH$_2$*C*H_2), 1.77 (brs, 2H, N$^+$CH$_2$*C*H_2), 2.00−2.25 (m, 2H, OCOCH$_2$*C*H_2 in Glu), 2.35−2.50 (m, 4H, NCOCH_2 and OCOCH_2 in Glu), 3.00−3.20 (m, 4H, CH_2Ar in Phe), 3.28 (s, 9H, N$^+$(CH_3)$_3$), 3.50−3.58 (brm, 2H, N$^+$CH_2), 4.00−4.10 (m, 4H, 2COOCH_2), 4.45−4.51 (m, 1H, CH in Glu), 4.64−4.80 (m, 2H, 2CH in Phe), 7.15−7.25 (m, 10H, Ar−H in Phe), 7.50 (brs, 1H, NH in Glu or Phe), 8.35 (brs, 1H, NH in Glu or Phe), 8.65 (brs, 1H, NH in Glu or Phe). This spectrogram was shown in ref 5. Anal. Calcd for $C_{61}H_{103}N_4O_7Br\cdot 2H_2O$: C, 65.39; H, 9.63; N, 5.00. Found: C, 65.31; H, 9.66; N, 4.99.

6: recrytallized from acetone; a colorless powder; mp 100.0−101.8 °C; IR (1 mM of CCl_4 solution) ν(N−H) 3280 cm^{-1}, ν_{as}(CH_2) 2926 cm^{-1}, ν_s(CH_2) 2854 cm^{-1}, ν(C═O, ester) 1737 cm^{-1}, ν(C═O, amide I) 1632 cm^{-1}, δ(N−H, amide II) 1543 cm^{-1}; ^{1}H NMR (60 MHz, $CDCl_3$) δ 0.88 (t, J = 7 Hz, 6H, 2CH_3 in long chain), 1.10−1.50 (brm, 54H, 27CH_2 in long chain), 1.77 (brm, 2H, N$^+$CH$_2$*C*H_2), 2.00−2.80 (brm, 10H, OCO*C*H_2*C*H_2 in Glu, S*C*H_2*C*H_2 in Met and NCOCH_2), 2.10 (s, 6H, 2SCH_3), 3.40 (s, 9H, N$^+$(CH_3)$_3$), 3.50 (s, 2H, N$^+$CH_2), 3.90−4.27 (brm, 4H, 2COOCH_2), 4.38−4.90 (brm, 3H, 3CH in Glu and Met), 7.17 (brs, 1H, NH in Glu or Met), 7.57 (brs, 1H, NH in Glu or Met), 7.75 (d, J = 6 Hz, 1H, NH in Glu or Met). Anal. Calcd for $C_{53}H_{103}N_4O_7S_2Br\cdot H_2O$: C, 59.47; H, 9.89; N, 5.23. Found: C, 59.22; H, 10.06; N, 5.10.

7: recrytallized from acetone; a colorless powder; mp 145.0−152.0 °C; IR (1 mM of CCl_4 solution) ν(N−H) 3264 cm^{-1}, ν_{as}(CH_2) 2927 cm^{-1}, ν_s(CH_2) 2855 cm^{-1}, ν(C═O, ester, see Figure 2) 1738 cm^{-1}, ν(C═O, amide I, see Figure 2) 1634 cm^{-1}, δ(N−H, amide II, see Figure 2) 1543 cm^{-1}; ^{1}H NMR (60 MHz, $CDCl_3$) δ 0.70−1.10 (brm, 18H, 2CH_3 in long chain, 2CH_3 in Val and 2CH_3 in Leu), 1.15−1.60 (brm, 54H, 27CH_2 in long chain), 1.60−2.10 (br, 6H, N$^+$CH$_2$*C*H_2, *C*H_2CH-(CH$_3$)$_2$ in Leu, OCOCH$_2$*C*H_2 in Glu), 2.10−2.70 (brm, 4H, NCOCH_2 and OCOCH_2 in Glu), 2.75−3.15 (brm, 2H, *C*H(CH$_3$)$_3$ in Val and CH$_2$*C*H(CH$_3$)$_2$ in Leu), 3.38 (s, 9H, N$^+$(CH_3)$_3$), 3.40 (s, 9H, N$^+$(CH_3)$_3$), 3.50 (s, 2H, N$^+$CH_2), 3.90−4.30 (brm, 4H, 2COOCH_2), 4.30−4.70 (m, 3H, 3CH in Glu, Val, and Leu), 6.65 (brs, 1H, NH in Glu, Val, or

Leu), 6.79 (brs, 1H, NH in Glu, Val, or Leu), 7.10 (brs, 1H, NH in Glu, Val, or Leu). Anal. Calcd for $C_{54}H_{105}N_4O_7Br\cdot 3H_2O$: C, 61.40; H, 10.59; N, 5.30. Found: C, 61.61; H, 10.65; N, 5.32.

9: recrytallized from a mixture of chloroform and hexane; a colorless powder; mp 159.2−164.9 °C; IR (CCl_4 solution) ν(N−H), ν(C−H), ν(C═O, ester) 1740, ν(C═O, amide I), δ(N−H, amide II), ν(C−C−O, ester) cm^{-1}; ^1H NMR (60 MHz, $CDCl_3$) δ 0.80 (brt, 3H, CH_3 in long chain), 1.00−1.95 (brm, 42H, $18CH_2$ in long chain and $2CH_3$ in Ala), 2.00−2.40 (brm, 2H, $NCOCH_2$), 3.35 (s, 9H, $N^+(CH_3)_3$), 3.55 (brs, 2H, N^+CH_2), 3.90−4.20 (brm, 2H, $COOCH_2$), 4.20−4.70 (brm, 3H, 3CH in Ala), 7.35 (brs, 1H, NH in Ala or Glu), 7.53 (brs, 1H, NH in Ala or Glu), 7.67 (brs, 1H, NH in Ala or Glu). Anal. Calcd for $C_{35}H_{69}N_4O_5Br\cdot{}^9/_4H_2O$: C, 56.32; H, 9.93; N, 7.51. Found: C, 56.37; H, 9.65; N, 7.76.

10: recrytallized from acetone; a colorless powder; mp 178.3−182.7 °C; IR (1 mM of CCl_4 solution) ν(N−H) 3279 cm^{-1}, $\nu_{as}(CH_3)$ 2961 cm^{-1}, $\nu_{as}(CH_2)$ 2927 cm^{-1}, $\nu_s(CH_3)$ 2874 cm^{-1}, $\nu_s(CH_3)$ 2855 cm^{-1}, ν(C═O, ester) 1737 cm^{-1}, ν(C═O, very small intensity of nonbonding amide I) 1661 cm^{-1}, ν(C═O, bonding amide I) 1632 cm^{-1}, δ(N−H, amide II) 1545 cm^{-1}; ^1H NMR (60 MHz, $CDCl_3$) δ 0.60−1.05 (brm, 21H, CH_3 in long chain and 3CH(CH_3)CH_2CH_3 in Ile), 1.03−2.00 (brm, 42H, $18CH_2$ in long chain and 3CH(CH_3)CH_2CH_3 in Ile), 2.10−2.45 (brs, 2H, $NCOCH_2$ and $OCOCH_2$), 3.05 (brs, 3H, 3CH(CH_3)CH_2CH_3 in Ile), 3.40 (s, 11H, $CH_2N^+(CH_3)_3$), 3.80−4.24 (m, 2H, $COOCH_2$), 4.24−4.75 (brm, 3H, 3CH in Ile), 7.00−7.80 (br 3H, NH in Ile). Anal. Calcd for $C_{44}H_{87}N_4O_5Br\cdot{}^5/_4H_2O$: C, 61.84; H, 10.56; N, 6.56. Found: C, 61.92; H, 10.79; N, 6.44.

11: recrytallized from ethyl acetate; a colorless powder; mp 97.0−101.0 °C; IR (1 mM of CCl_4 solution) ν(N−H) 3282 cm^{-1}, $\nu_{as}(CH_2)$ 2926 cm^{-1}, $\nu_s(CH_2)$ 2854 cm^{-1}, ν(C═O, ester) 1738 cm^{-1}, ν(C═O, amide I) 1638 cm^{-1}, δ(N−H, amide II) 1544 cm^{-1}; ^1H NMR (60 MHz, $CDCl_3$) δ 0.85 (brt, 3H, CH_3 in long chain), 1.05−1.70 (brm, 34H, $17CH_2$ in long chain), 1.81 (brs, 2H, $N^+CH_2CH_2$), 2.00−2.50 (brm, 2H, $NCOCH_2$), 2.80−3.20 (brm, 6H, $3CH_2Ar$), 3.30 (s, 9H, $N^+(CH_3)_3$), 3.40−3.70 (brm, 2H, N^+CH_2), 3.75−4.20 (brm, 2H, $COOCH_2$), 4.25−4.80 (brm, 3H, 3CH in Phe), 6.55 (brs, 1H, NH in Phe), 6.90− 7.30 (m, 16H, 3Ar−H in Phe and NH in Phe), 7.75 (brs, 1H, NH in Phe). Anal. Calcd for $C_{53}H_{81}N_4O_5Br\cdot{}^5/_2H_2O$: C, 65.01; H, 8.85; N, 5.72. Found: C, 65.03; H, 8.94; N, 5.75.

12: recrytallized from ethyl acetate; a colorless powder; mp 90.5−93.2 °C; IR (1 mM of CCl_4 solution) ν(N−H) 3271 cm^{-1}, $\nu_{as}(CH_2)$ 2926 cm^{-1}, $\nu_s(CH_2)$ 2854 cm^{-1}, ν(C═O, ester, see Figure 6) 1739 cm^{-1}, ν(C═O, very small intensity of nonbonding amide I, see Figure 6) 1663 cm^{-1}, ν(C═O, bonding amide I, see Figure 6) 1638 cm^{-1}, δ(N−H, amide II, see Figure 6) 1541 cm^{-1}; ^1H NMR (500 MHz, $CDCl_3$) δ 0.88 (t, J = 7 Hz, 3H, $2CH_3$ long chain) 1.15−1.33 (m, 26H, $13CH_2$ in long chain), 1.36 (brs, 2H, $N^+CH_2CH_2CH_2$), 1.42−1.50 (m, 2H, $NCOCH_2CH_2$), 1.51−1.58 (brm, 2H, $COOCH_2CH_2$), 1.72 (brs, 2H, $N^+CH_2CH_2$), 2.12 (t, J = 7.3 Hz, 2H, $NCOCH_2$), 2.96 (d, J = 7 Hz, 2H, CH_2Ar), 2.99 (d, J = 7.3 Hz, 2H, CH_2Ar), 3.03−3.13 (m, 2H, CH_2Ar), 3.30 (s, 9H, $N^+(CH_3)_3$), 3.42−3.48 (m, 2H, N^+CH_2), 3.95−4.15 (m, 2H, $COOCH_2$), 4.56 (d, t, J = 7 Hz, J = 7 Hz, 1H, CH in Phe), 4.57 (d, t, J = 7 Hz, J = 7 Hz, 1H, CH in Phe) 4.69 (d, t, J = 7 Hz, J = 7 Hz, 1H, CH in Phe), 6.67 (d, J = 8 Hz, 1H, NH in Phe), 7.01 (d, J = 7.4 Hz, 1H, NH in Phe), 7.10−7.30 (m, 15H, 3Ar−H in Phe), 7.39 (d, J = 8.2 Hz, 1H, NH in Phe). Anal. Calcd for $C_{53}H_{81}N_4O_5Br\cdot{}^1/_2H_2O$: C, 67.49; H, 8.76; N, 5.94. Found: C, 67.27; H, 8.95; N, 5.88.

FT-IR Measurements. The sample solutions were prepared by sonication. In cases of binary systems, components were mixed in $CHCl_3$, and the solvent was evaporated. The mixed film thus obtained was dissolved in CCl_4 by sonication. The sample solution was sandwiched between the CaF_2 windows with a 19-μm spacer for $CHCl_3$ and CCl_4 solutions and a 50-μm spacer for the aqueous solution. The CaF_2 windows were mounted in a temperature-controlled flow-through cell (Harrick Scientific Co., TFC-M19). The IR spectra were recorded on a Nicolet 740 Fourier transform infrared spectrometer with a TGS detector at 25 ± 0.5 °C. Two hundred interferograms were co-added and Fourier transformed with one level of zero filling to yield spectra with a high S/N ratio at a resolution of 4 cm^{-1}.

TEM Measurements. The staining of aggregates in organic solvents was carried out in the same manner as that described in ref 10. A sample solution (2 mM) was dropped onto a carbon-coated TEM grid. Excess liquid was blotted off and the residue dried in vacuo. The observation was carried out with a JEOL JEM 100S transmission electron microscope.

AFM Measurements. The AFM observation was carried out for the cast films from different solutions on freshly cleaved mica. The AFM images were taken by a Nanoscope IIIa (Digital Instruments, Santa Barbara, CA) in a tapping mode in air. According to the manufacturer, the normal spring constant was 20−100 N/m. Drive frequency was around 300 kHz. Scanning speed was at a line frequency of 1 Hz with 256 pixels per line.

Results and Discussion

The amphiphiles used in the study formed an aggregate not only in water but also in some nonpolar organic solvents.[5−7] On the other hand, they formed no aggregate in polar solvents such as ethanol and chloroform. The aggregation behavior can be monitored by vibrational spectroscopy because the aggregation of the peptides is accompanied by band shifts from a nonbonding to a characteristic amide bonding mode.[6] The nonbonding amide modes at 3412−3426 cm^{-1} (amide A), 1659−1678 cm^{-1} (amide I), and 1503−1516 cm^{-1} (amide II) were observed in the $CHCl_3$ solutions without respect to the tripeptide structure, whereas the amide bonding modes were observed in aqueous solutions and in CCl_4 solutions (Table 1).

The FT-IR spectra of these bonding bands were divided into four types as shown in Figure 2. The type I spectrum is the most ordinary structure in the present study, where amide A absorbed at 3271−3285 cm^{-1}, amide I only absorbed at 1631−1638 cm^{-1} and amide II at 1536−1547 cm^{-1}. Amide A and amide I are more than 100 and 20 cm^{-1} lower, respectively, than those observed in $CHCl_3$ solution. Amide II, a deformation mode of N−H, is 20 cm^{-1} higher than that observed in $CHCl_3$. Furthermore, the half bandwidths of the bonding amide I bands were ca. 12 cm^{-1}, which were 30 cm^{-1} smaller than that of the nonbonding amide I bands in $CHCl_3$ solution (ca. 50 cm^{-1}). These results show that a strong and orderly hydrogen bond was formed in the aggregate of these amphiphiles. According to a previous report, *N*-deblocked-heptavaline, heptaisoleucine, and heptaphenylalanine, which adopted a parallel β-sheet alignment in the crystal, showed the same amide mode because amide I and amide II appeared at 1635−1639 cm^{-1} and 1540−1549 cm^{-1}, respectively, and no other peaks appeared in the region.[11] Therefore, the tripeptide-containing amphiphiles except for **1** and **2** should form the parallel β-sheet structure in the aggregate without respect to whether the solvent is aqueous or organic.

The formation of the parallel β-sheet is explained from a morphological aspect. Possessing a hydrophilic head and hydrophobic chains, the amphiphiles formed a normal bilayer structure (Figure 1a) in water.[8] An interdigitated monolayer structure (Figure 1c) is unfavorable in water because the hydrophilic ammonium head is buried in the hydrophobic chain region. The structure is possible only in the organic media. However, we observed a fibrous structure in CCl_4 solutions of the tripeptide-containing amphiphiles by transmission electron microscopy. For example, Figure 3 is the TEM image of **2** in three different organic solvents. Small fibers observed in these images have a 70−80 Å diameter. Because the expanded length of the molecule is 45 Å, the diameter corresponds to the

(10) Ishikawa, Y.; Kuwahara, H.; Kunitake, T. *J. Am. Chem. Soc.* **1994**, *116*, 5579−5591.

(11) Toniolo, C.; Palumbo, M. *Biopolymers* **1977**, *16*, 219−224.

Table 1. Absorption Frequencies of Tripeptide Molecules in Different Media

tripeptide molecules	solvents[a]	spectral type[b]	frequencies/cm^{-1} amide A	amide I	amide II
1	CCl_4	IV	3366, 3319	1677, 1663, 1649	1537, 1513
	water	E	*c*	1650	1549
2	$CHCl_3$ (5 mM)	N	3414	1661	1503
	CCl_4	III	3299	1647, 1631	1560, 1534
	water	III	*c*	1647, 1632	1561, 1534
3	CCl_4	I	3280	1632	1546
4	CCl_4	I	3281	1632	1546
5	$CHCl_3$ (16 mM)	N	3412	1668	1518
	CCl_4	I	3282	1637	1542
	water	I	*c*	1638	1538
6	CCl_4	I	3280	1631	1543
7	$CHCl_3$	N	3420	1664	1516
	CCl_4	I	3285	1634	1543
	water	I	*c*	1635	1544
8	$CHCl_3$ (20 mM)	N	3420	1678	1504
	CCl_4 (10 mM)	II	3277	1688, 1630	1527
	water		insoluble	insoluble	insoluble
9	CCl_4		precipitate	precipitate	precipitate
	water	I	*c*	1634	1547
10	$CHCl_3$	N	3426	1659	1505
	CCl_4	I	3279	1632	1545
	water	I	*c*	1633	1548
11	CCl_4	I	3282	1636	1545
	water	I	*c*	1637	1536
12	CCl_4	I	3271	1638	1541

[a] Concentrations of the sample solutions were 1 mM for $CHCl_3$ and CCl_4 solution and 20 mM for aqueous solutions. [b] N and E denote a nonbonding amide mode and a specific mode except for a β-sheet structure (see text), respectively, and the others (I−IV) are classified according to Figure 2. [c] It is impossible to subtract the solvent absorption in this region because of the strong ν(O−H) band of water. Measurement temperature was 25.0 ± 0.5 °C. The other conditions are cited in parentheses.

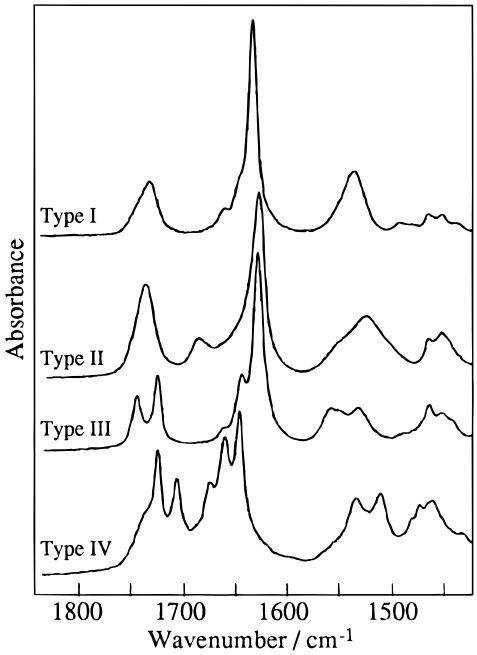

Figure 2. FT-IR spectra of four different types of secondary structures of tripeptide derivatives: type I (parallel β-sheet), CCl_4 solution of **7** (1 mM); type II (antiparallel β-sheet), CCl_4 solution of **8** (10 mM); type III (pseudoparallel β-sheet), CCl_4 solution of **2** (1 mM); type IV, CCl_4 solution of **1** (1 mM). All spectra were measured at 25.0 ± 0.5 °C.

thickness of a reversed bilayer structure (Figure 1b) in which the components are slightly tilted. This result means that the local structure of the aggregate in organic solvents did not adopt an interdigitated structure (Figure 1c) but a reversed bilayer structure. The normal and reversed bilayer structures contain the same molecular alignment in their half-layer and hence contained the same parallel β-sheet structure.

The type II spectrum is attributed to a typical antiparallel β-sheet structure where amide I absorbs at 1630 cm^{-1}, together with a weak band at 1688 cm^{-1}, and amide II at 1527 cm^{-1}. The major band of amide I in the antiparallel β-sheet absorbed at a slightly lower frequency in comparison with that in the parallel β-sheet structure. The essential difference between the structures is whether the weak band at about 1690 cm^{-1} is present. This weak band has been inferred from the results of a theoretical calculation for the antiparallel β-sheet polypeptides[11,12] and observed in crystalline heptaalanine, heptanorvaline, heptaleucine, heptamethionine, and hepta-*S*-methylcysteine containing an antiparallel β-sheet structure.[11] In cases of the heptapeptides, the major amide I band also appeared at a lower frequency (1630−1633 cm^{-1}) than that of the peptides forming a parallel β-sheet structure (1635−1639 cm^{-1}). The type II spectrum was only observed in the CCl_4 solution of the hydrophobic Ala-Ala-Glu derivative **8**. In this case, the hydrophobic **8** should pack according to an interdigitated structure (Figure 1c).

The type III spectra were characteristic of Ala-Ala-Glu-containing amphiphile **2** in water and CCl_4, where the bands attributed to the ester, amide I and amide II split into two peaks. For example, the amide I band split into 1647 and 1631 cm^{-1} (Figure 2). The presence of the major peak at 1631 cm^{-1} and the absence of the weak band at about 1690 cm^{-1} indicate the formation of a parallel β-sheet conformation. However, the band split, particularly at the ester carbonyl, suggests that one of the amide groups forms a hydrogen bond with either an α- or a γ-ester group. We call this specific amide mode a pseudoparallel β-sheet structure.

The type IV spectrum was observed in the CCl_4 solutions of Gly-Gly-Glu-containing amphiphile **1**. The multiple peaks assigned to the amide I band meant that the amphiphile did not form any β-sheet structures. The amphiphile gave different

(12) Bandekar, J. *Biochim. Biophys. Acta* **1992**, *1120*, 123−143.

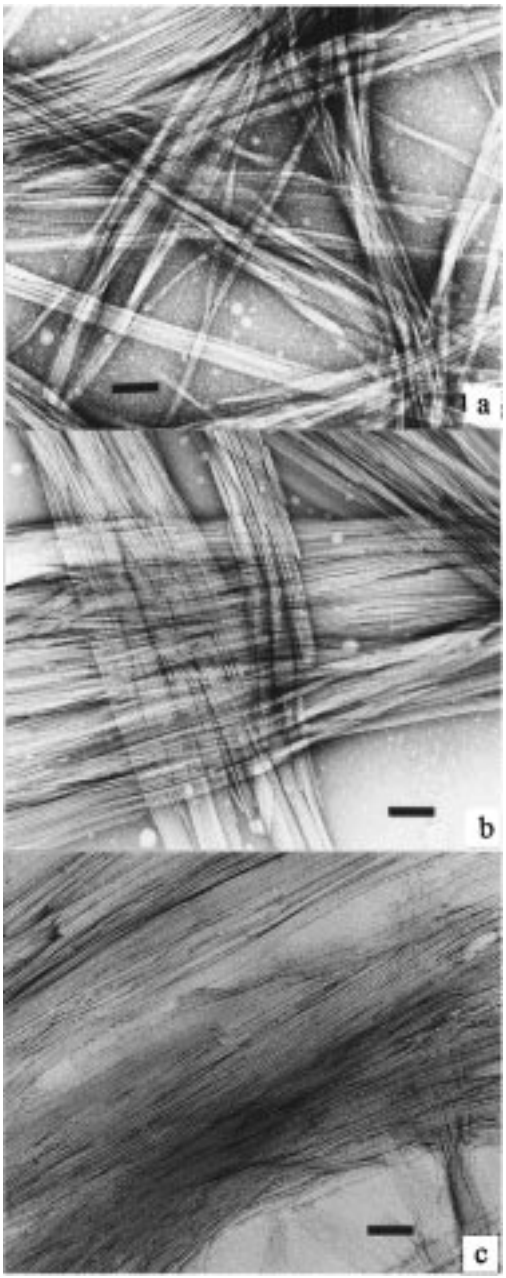

Figure 3. TEM images of the assemblage of **2** in three different solvents (scale bar; 1000 Å). (a) CCl_4, (b) benzene, (c) cyclohexane.

spectra depending upon the conditions. In this aggregate, the H-bonding could be formed two-dimensionally because glycinate residues possessed no sterically hindered side group.

The respective FT-IR spectra (types I, II, and III) of the solutions of the tripeptide-containing amphiphiles remained unchanged when the solutions were diluted or condensed to dryness. For example, the type I amide mode of Phe-Phe-Glu **5** was unchanged in CCl_4 solution at 25 °C even if the concentration decreased to 0.01 mM which is the lower limit of detection. Therefore, the critical concentration of the aggregate formation of **5** is lower than 0.01 mM in CCl_4 at 25 °C. Heating also caused no spectral change. Figure 4 is an example of the temperature dependence of FT-IR spectra observed in the CCl_4 solution of **3**. The spectra remained unchanged if the temperature was raised to 60 °C, although we did not measure the sample at a still higher temperature because of the difficulty with temperature control. These results show that the aggregate possesses a thermal stability, which is very

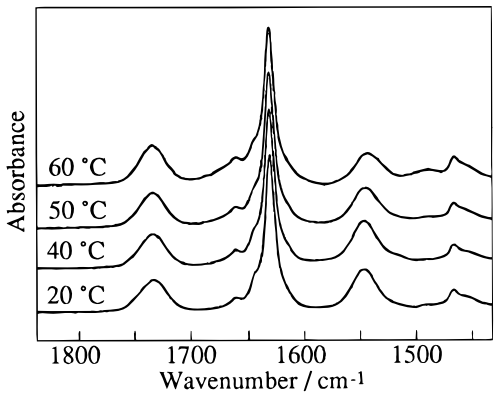

Figure 4. Temperature dependence of FT-IR spectra of **3** in CCl_4 solution.

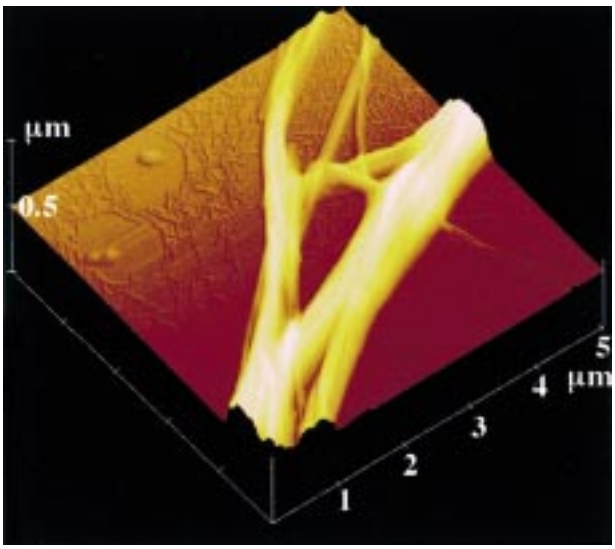

Figure 5. AFM image of the air-dried cast film from CCl_4 solution of **2**.

similar to that of the amyloid filaments. On the other hand, isotropic $CHCl_3$ solution, which showed a nonbonding amide mode, gave the type I spectra when the solvent was removed to dryness (Table 2). In particular, that of the amphiphile **2** was characteristic. The $CHCl_3$ solution of **2** produced the type I spectrum, a parallel β-sheet, after air-drying even if the air-dried film from CCl_4 produced the type III spectrum, a pseudoparallel β-sheet. Therefore, we obtained a pseudoparallel, a parallel, and an antiparallel β-sheet, by modifying the chemical structure, changing the solvent, and/or drying the solutions.

The light intensity at the nonbonding amide I band (1659−1678 cm^{-1}) within the spectra of the β-sheets (Figures 2 and 4) shows that the β-sheets should extend for a long period. In fact, transmission electron microscope (TEM) pictures revealed well-developed filaments whose diameters are 70−80 Å (Figure 3). The direction of all of the tripeptide chains should be oriented perpendicularly to the axis of the filament, which corresponds with the Alzheimer's β-peptide in which the peptide is perpendicular to the fiber axis.[13] These filaments assembled into a bundle, which can be observed three-dimensionally using AFM. Although AFM is now widely used for various objects on a μm to sub-μm scale as well as for observations at the molecular level,[14] observations at the sub-μm level have been

(13) Kirschner, D. A.; Inouye, H.; Duffy, L. K.; Sinclair, A.; Lind, M.; Selkoe, D. J. *Proc. Natl. Acad. Sci. U.S.A.* **1987**, *84*, 6953−6957.

(14) Shao, Z.; Mou, J.; Czajkowsky, D. M.; Yuan, J.-Y. *Adv. Phys.* **1996**, *45*, 1−86.

Table 2. Absorption Frequencies of Air-Dried Cast Films of Tripeptide Molecules

tripeptide molecules	solvents[a]	spectral type[a]	frequencies/cm^{-1}		
			amide A	amide I	amide II
1	CCl_4	E	3364, 3320	1674, 1663	1536, 1516
2	$CHCl_3$	I	3301	1631	1542
	CCl_4	III	3301	1647, 1631	1559, 1533
3	$CHCl_3$	I	3279	1635	1545
	CCl_4	I	3281	1634	1541
	water	I	3279	1633	1547
4	CCl_4	I	3280	1634	1544
5	$CHCl_3$	I	3287	1637	1539
	CCl_4	I	3286	1637	1538
	water	I	3287	1637	1538
7	ethyl acetate	I	3281	1634	1543
	water	I	3284	1634	1544
8	$CHCl_3$	II	3277	1686, 1628	1537
	CCl_4	II	3277	1689, 1628	1535

[a] E denotes a specific mode except for a β-sheet structure (see text), and the others (I−III) are classified according to Figure 2. Measurement temperature was 25.0 ± 0.5 °C.

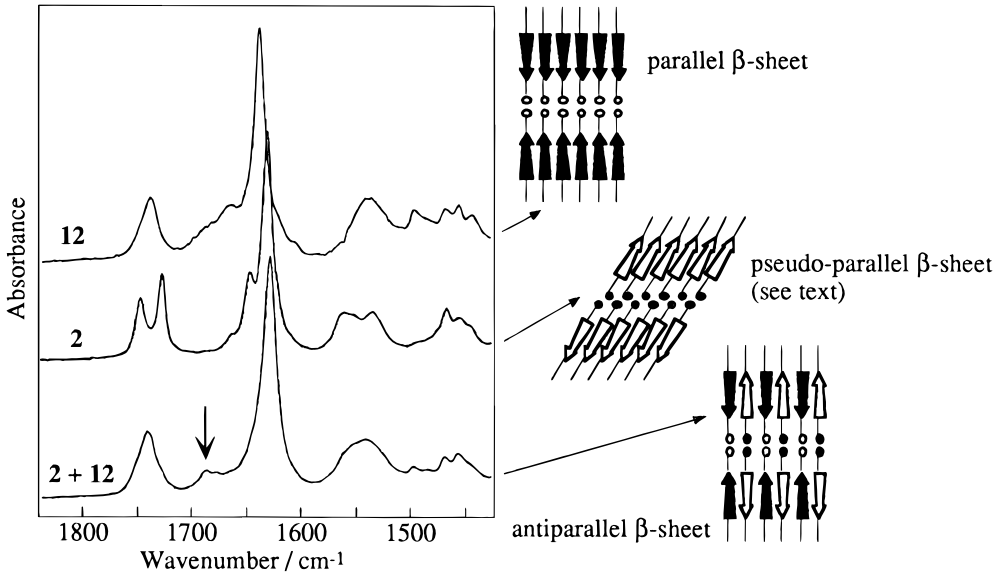

Figure 6. FT-IR spectra of binary mixture and respective components (**2** and **12**) in CCl_4 solution. Band split of **2** disappeared and a weak band appeared at 1686 cm^{-1} (arrow at the bottom spectrum), which means the formation of an antiparallel β-sheet structure.

slighted despite their usefulness. Amyloid-like filaments whose diameters varied from a few nanometers to 1 μm were depicted in the AFM image. Figure 5 is a typical example of the AFM image of the cast film from the CCl_4 solution of **2**, whose secondary structure was a pseudoparallel β-sheet as previously described. It is important that the similar outsides were obtained using TEM and AFM, even if the samples were prepared by the different procedures. The TEM sample was adsorbed fibers onto an amorphous carbon film, whereas the AFM sample was a dried specimen of an organogel on mica. We can observe several branches in a tapping mode AFM image, whose widths and height were 10−30 nm and 10−20 nm, respectively. The most narrow branch should be an isolated fiber because the diameter of the fiber evaluated from TEM images was 7−8 nm. Although it was difficult to distinguish the respective β-sheet structures from each other, namely, pseudoparallel- and parallel-chain β-sheet structures, only from the AFM images, it is noteworthy that a three-dimensional image of the β-sheet assemblage can be visualized because such a three-dimensional image has not yet been reported. The detailed morphological aspect of the sub-μm AFM imaging is under experimental study.

The AFM and the TEM results showed that the tripeptide-containing molecules formed a β-sheet assemblage. A similar structure was observed within the cast films of amphiphiles containing the other tripeptide residues. As previously described, all of the amphiphiles except for **1** formed a parallel β-sheet structure despite the large structural difference. However, the parallel β-sheet could be transformed into an antiparallel counterpart when the molecule was mixed with another tripeptide-containing amphiphile **12** whose tripeptide part has an opposite direction. For example, when the tripeptide-containing amphiphile **2** was mixed with the single chain amphiphile **12**, a weak band at 1686 cm^{-1}, which is evidence of an antiparallel β-sheet, appeared together with a strong amide I band at 1629 cm^{-1} similar to that of the tripeptide molecule **8** (Figure 6). The amphiphile **12** alone, of course, formed a parallel β-sheet. On the other hand, it was possible to reform the pseudoparallel β-sheet structure of **2** into a parallel β-sheet structure. In this case, the pseudoparallel β-sheet structure of **2** transformed into a parallel β-sheet structure, on mixing with a parallel β-sheet-forming **5** or **9**. The transformations between secondary structures are associated with the natural amyloid formation, because it is believed that a segment of a protein in the β-sheet form, especially a prion peptide, catalyzes the further conversion of segments from an α-helix to the β-sheet form.[1,15]

(15) Gasset, M.; Baldwin, M. A.; Lloyd, D. H.; Gabriel, J.-M.; Holtzman, D. M.; Cohen, F.; Fletterick, R.; Prusiner, S. B. *Proc. Natl. Acad. Sci. U.S.A.* **1992**, *89*, 10940−10944.

Conclusions

There is controversy concerning the amide modes due to parallel β-sheet conformation because of the model polypeptide's lack of known X-ray structure for this conformation.[12] Hence whether a β-sheet is parallel or antiparallel has not been rigorously examined. Also, an interconversion between the two structures has not been attempted. Here we demonstrated that most of the tripeptide-containing amphiphiles formed a parallel β-sheet structure in their assemblages. Emphasis is placed on the controllability of the β-sheet structure within the assemblage. The parallel β-sheet structure can be transformed into an antiparallel counterpart by modifying the chemical structure, changing the solvent, and mixing with other tripeptide molecules possessing an opposite direction. It is sometimes difficult to study amide modes when a tripeptide itself was used because the intermolecular H-bonding between the amino group and the carboxyl group appeared in the amide I region. The presence of a protective group on the amino group also disturbs the detection of the amide I bands. On the other hand, the tripeptide-containing amphiphiles self-organized into a parallel β-sheet assemblage, in which no H-bonding other than that between the peptide linkages was present. Therefore, the present assemblage should be a good model for the β-sheet polypeptides. Morphological similarity also suggests that the fibrous model including a parallel β-sheet structure should be helpful in studying the structure and function of abnormal peptides such as the prion and the amyloid.

Acknowledgment. We thank Professor Yoshio Okahata, Department of Biomolecular Engineering, Tokyo Institute of Technology, for the AFM observations. This work was supported in part by a Grant-in-Aid for Scientific Research (No. 970018) from the Futaba Electronics Memorial Foundation, Chiba, Japan.

JA981363Q